

## Abstract

Polyamides composed of N-methylimidazole (Im), N-methylpyrrole (Py), and 3-hydroxy-N-methylpyrrole (Hp) are minor groove-binding ligands capable of specific recognition of predetermined DNA sequences. Decades of research in this field has yielded several motifs for DNA recognition with affinities and specificities comparable to naturally occurring proteins. Hairpin polyamides, in particular, have been used extensively in biological applications and may ultimately prove valuable as therapeutic agents; however, the full potential of these molecules is still inherently limited by the physical properties of the thymine-specific Hp residue.

Efforts to expand the repertoire of sequences available to polyamide recognition have included the design of new polyamide motifs as well as the development of novel thymine-specific residues for Hp replacement in both *N-terminal* and *internal* pairings. One approach to novel residues has focused on removing the hydroxyl recognition element of Hp in favor of purely shape selective thymine discrimination by the sulfur atom of thiophene heterocycles. An alternative strategy replaced the unstable pyrrolyl hydroxyl group with a more chemically robust phenol. Both approaches have shown promise in the context of single novel pairing with Py, in a model hairpin polyamide, and both Tn and Hz are more stable than Hp.

Determination of the efficacy of Tn and Hz in targeting multiple T•A base pairs in a single polyamide were evaluated by quantitative DNase I footprinting titrations on a designed plasmid. This data suggests that Hz/Py pairings, which show comparable specificities and higher affinities relative to Hp/Py pairings, might be effective in biological applications.

## Background and Significance

Seminal efforts toward the development of minor groove-binding polyamides focused on engineering G•C specificity into the T, A selective natural products distamycin A and netropsin. This goal was eventually realized by a single atomic substitution, replacing the C3H of N-methylpyrrole (Py) with N to give N-methylimidazole (Im).<sup>1,2</sup> The specificity of these first generation polyamides was attributed to side-by-side pairings of Im with Py such that Im/Py targets G•C and Py/Im targets C•G, using hydrogen bonding between the N3 of Im and the exocyclic amine of guanine as a physical basis for discrimination in the minor groove.<sup>3</sup> Py/Py pairings, on the other hand, are degenerate for T•A and A•T, owing to the similarity of these base pair edges in the minor groove.<sup>4,5</sup>

Second generation polyamides incorporated a third aromatic residue, 3-hydroxy-N-methylpyrrole (Hp), for thymine recognition.<sup>6</sup> This new heterocycle was also created by a single atomic substitution, replacing the C3H of Py with the hydroxyl recognition element of Hp. Pairings of Hp with Py completed the DNA recognition code for minor groove-binding polyamides, allowing T•A and A•T to be targeted by Hp/Py and Py/Hp pairings, respectively. The molecular basis for thymine recognition by Hp consists of electronic and steric components.<sup>7</sup> Hydrogen bond donation by the hydroxyl group of Hp, though energetically favorable with the divalent thymine O2 acceptor, is not possible with the monovalent adenine N3 acceptor. The bulky nature of the Hp hydroxyl moiety also distinguishes the asymmetric cleft of T•A base pairs, preferring to lie over the less sterically demanding thymine ring.

The molecular details of DNA recognition described above are collectively referred to as the *pairing rules*, and while these principles have guided the design of polyamides targeting hundreds of predetermined DNA sequences with high affinities and specificities, inherent limitations of Hp have restricted their generality. Hp-containing polyamides often show reduced binding affinities relative to their Py counterparts, possibly as a result of intramolecular hydrogen bonding between the hydroxyl group of Hp with the preceding amide proton, resulting in weaker association of the polyamide strand with the minor groove floor. Computational studies have indicated that desolvation of the Hp hydroxyl group upon insertion into the minor groove might contribute to reduced association constants.<sup>8</sup> Hp has also shown limited stability in aqueous solutions, owing to decomposition through acid- and radical-mediated mechanisms. The above effects are magnified when binding sites containing multiple T•A /A•T base pairs are to be targeted specifically with reasonable affinities.<sup>9,10</sup>

Efforts to develop novel internal residues have been guided by the mechanism of Hp-based thymine discrimination as well as by physical studies on N-terminal recognition. Two fundamental strategies for the design of Hp replacements have been explored by biophysical studies. One approach removes the hydroxyl recognition element altogether, relying on purely shape selective recognition of the asymmetric cleft for thymine-specificity. The N-terminal residues discussed in Chapter 5 and their internal, 3-methylthiophene (Tn) forerunner were designed using this strategy.<sup>11,12</sup> A second approach replaces the unstable pyrrolyl hydroxyl group

with a more chemically robust phenol, as in the case of hydroxybenzimidazole (Hz).<sup>13-15</sup>

Novel internal residues are incorporated into a model hairpin polyamide containing strategically placed Im/Py pairs to ensure that the novel residue lies over the variable base pair in the binding site cassette. Two plasmids, complementary to the N-terminal plasmid used in Chapter 5, are typically employed to characterize the DNA-binding energetics of novel heterocycles by quantitative DNase I footprinting titrations (Figure 6.1). The first of these plasmids addresses the specificity of a single pairing for all four Watson-Crick base pairs, while the second examines the efficacy of two adjacent novel pairings in recognition of multiple T•A /A•T base pairs.

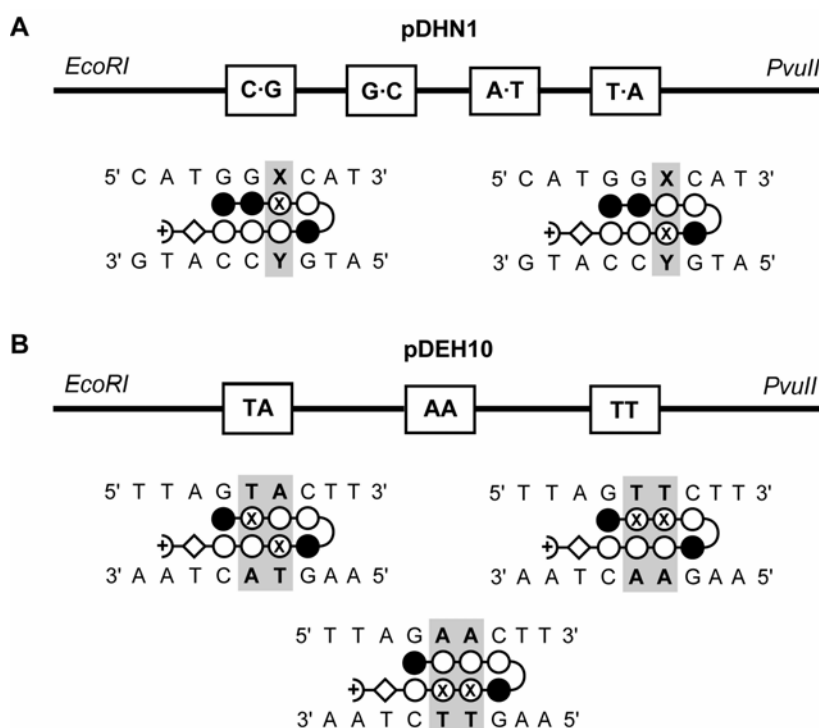


**Figure 6.1** Designed plasmids used to assess DNA binding properties of hairpin polyamides targeting internal or multiple thymine bases. **(A)** All four Watson-Crick base pairs are included at the X/Y position. **(B)** The central base pairs of the hairpin binding site are varied to include all adjacent T, A dinucleotide sequences.

### Fluorine as a Shape Selective Recognition Element—3-Fluoropyrrole

One of the earliest envisioned replacements for Hp was 3-fluoropyrrole. A fluorine substituent imposes steric demands comparable to a hydroxyl group, while eliminating potentially detrimental intramolecular hydrogen bonding interactions. Aromatic fluorides are also known to exhibit hydrophobic character, making insertion into the minor groove a favorable event.<sup>16</sup> Thus, 3-fluoropyrrole was expected to recognize T•A base pairs by a shape selective mechanism (Figure 6.2).

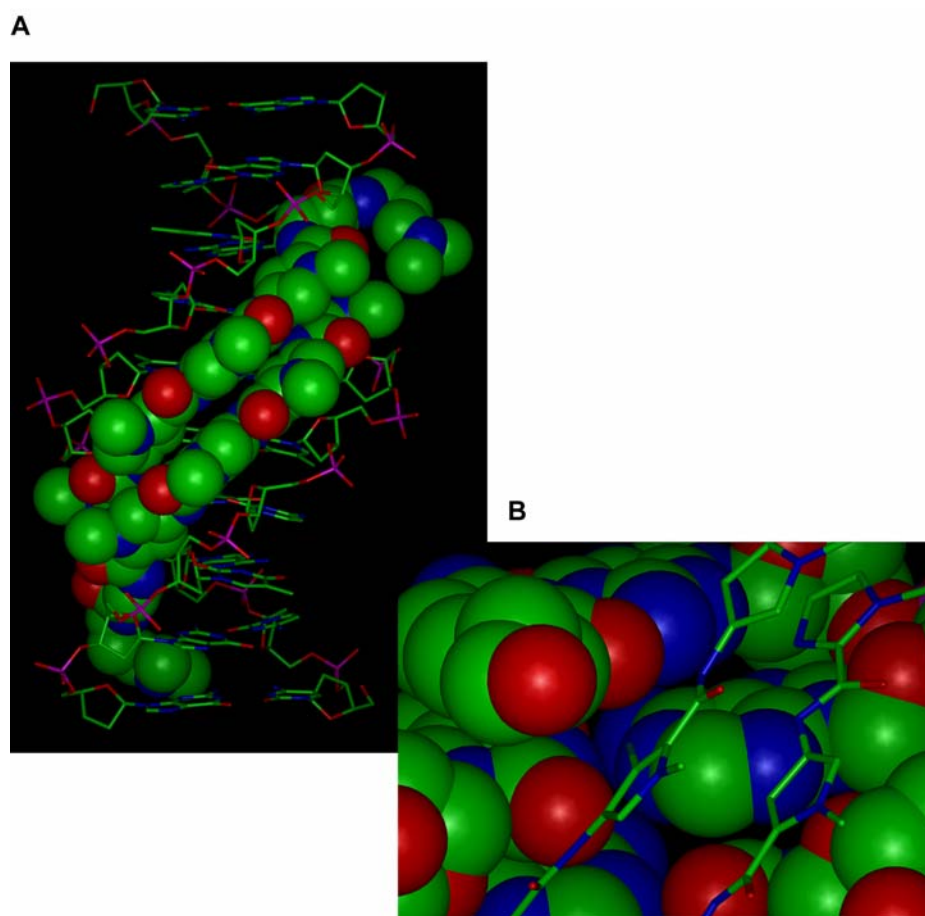


**Figure 6.2** Molecular rendering of a 3-fluoropyrrole-containing polyamide bound in the minor groove of DNA. **(A)** A polyamide homodimer is shown as a spacefilling model bound in the minor groove. **(B)** Blow up of the region of contact between the fluoropyrrole moiety and the base pair edges (shown as spacefilling model) on the floor of the minor groove.

Retrosynthetic analysis of the 3-fluoropyrrole building block (Fp) suggested three potential routes to key intermediate **1** using either nucleophilic or electrophilic methods of fluorination (Figure 6.3). Conversion of Hp precursor **2** to a sulfonate ester sets the stage for nucleophilic substitution by fluoride. This chemistry is often employed in industrial settings, requiring high temperatures to compensate for reduced nucleophilic character of fluoride. Alternatively, selective 3-bromination of N-methylpyrrole could be used to set up lithium-halogen exchange. Treatment of the lithium salt with an electrophilic source of fluorine would then afford a fluorinated starting material compatible with the existing synthetic scheme for Py. More reliable access to intermediates **3** and **4** can be obtained using N-(triisopropylsilyl)pyrrole (TIPS-Py) as a starting material. Steric shielding of the more reactive 2-position of the pyrrole ring has been used to prepare a range of 3-substituted pyrrole derivatives. With fluorinated pyrrole derivative **5** in hand, two schemes, varying the order of introduction of nitro and ester groups, could be explored.

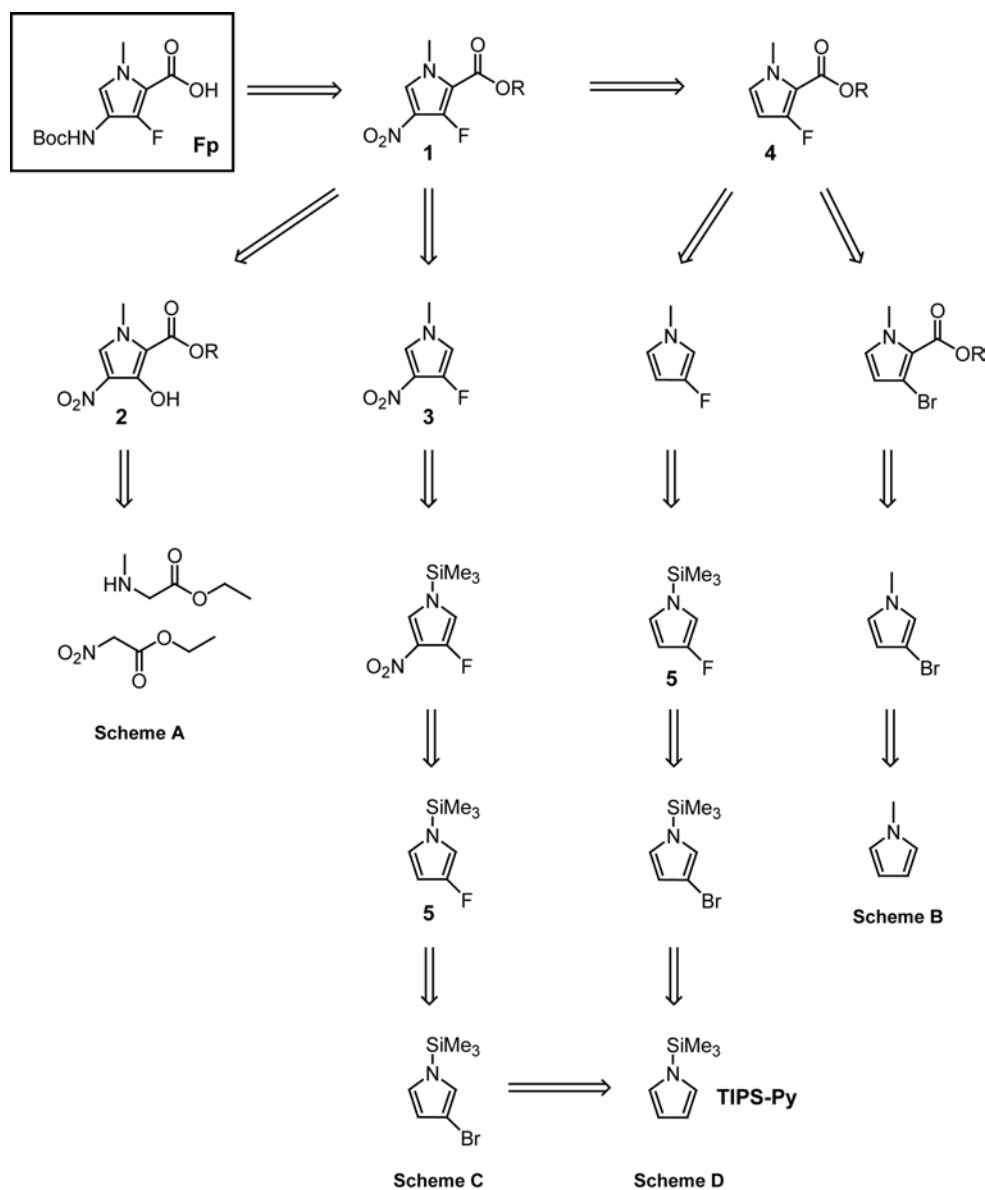


**Figure 6.3** Retrosynthetic analyses of 3-fluoropyrrole building block. Scheme A uses nucleophilic methods of fluorination while Scheme B-D employ electrophilic fluorination strategies.

Preliminary efforts toward the synthesis of Fp attempted direct fluorination of **2** with diethylamino sulfur trifluoride (DAST) without success. Activated sulfonates **7-9** were prepared by standard protocols; however, nucleophilic substitutions using

different fluoride sources, solvent systems, catalysts, and a range of temperatures all failed to give **10** in any appreciable yield (Figure 6.4A). There is precedent in the literature for instability of *o*-nitro aromatic fluorides, owing to destabilization of the nitro  $\pi$  system by the fluorine lone pairs.<sup>16</sup> In light of this, **6** was reacted with *t*BDMS-Cl to give **11**. Subsequent reduction, Boc-protection and desilylation with TBAF

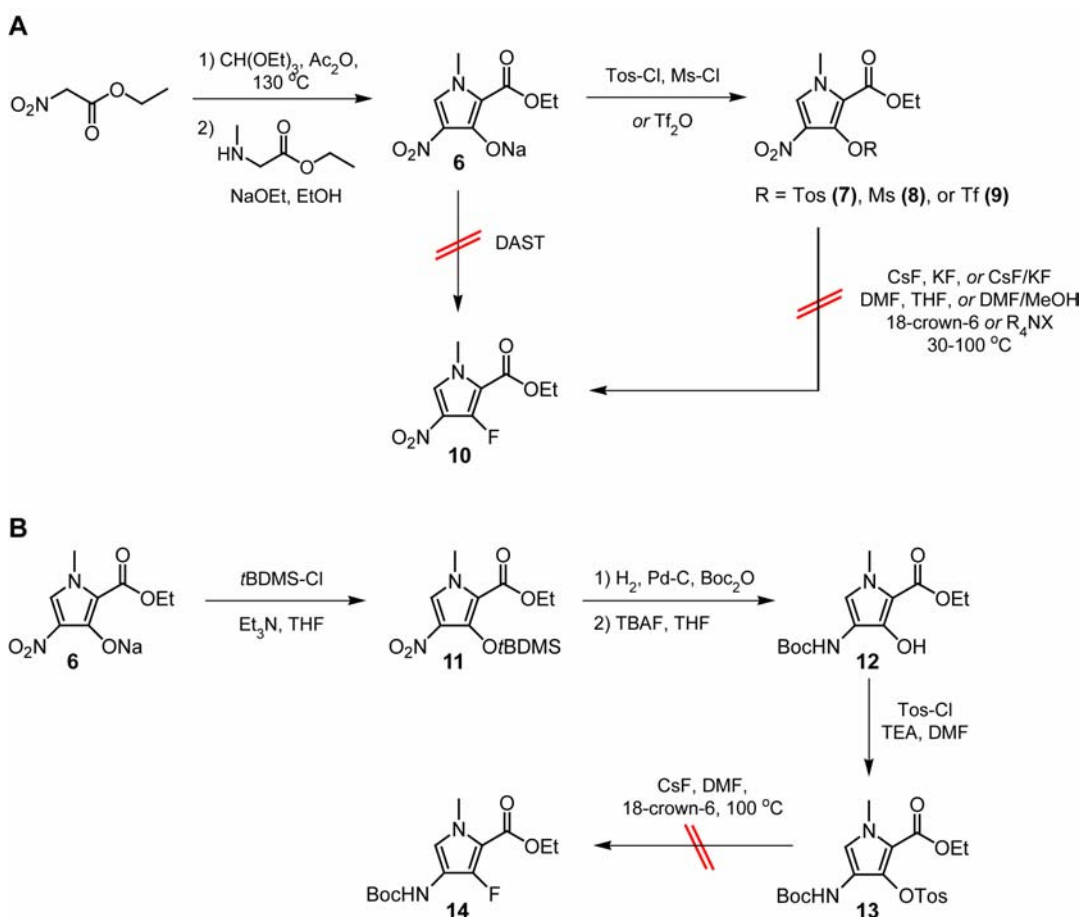


**Figure 6.4** Attempted routes to 3-fluoropyrrole building block using nucleophilic methods of aromatic fluorination. **(A)** Attempted early-stage fluorination of nitrated Hp precursor. **(B)** Attempted late-stage fluorination of Hp precursor.

afforded **12**, which was converted to the corresponding tosylate, **13**. Again a range of substitution conditions were examined but none yielded **14** (Figure 6.4B). Clearly, nucleophilic *halix* chemistry is not suited to the task at hand. Nitrated Py



derivatives, **7-9**, yield fluorinated products that also activated to further reaction, while late-stage fluorination of **13** was probably ineffective due to greater electron density of the aromatic ring.

Perhaps the mildest fluorination methods, described in the literature, use lithium halogen exchange, in conjunction with electrophilic N-F reagents, to prepare aryl fluorides from the corresponding bromides. The immense body of work concerning aromatic bromination combined with the inherent selectivity of lithium-halogen exchange reactions suggested that 3-bromo-N-methylpyrrole **16** could provide access to Fp with only slight modification to the existing scheme for Py.<sup>17-19</sup> Selective  $\beta$ -monobromination of the pyrrole nucleus is challenging, owing to the greater nucleophilicity of the  $\alpha$ -position; however, the preparation of **16** from N-methylpyrrole has been described. This route employs acid-catalyzed rearrangement of the more readily available,  $\alpha$ -brominated **15** install the 3-bromo group. This scheme proved effective on small scales (< 1g), but resulted in polymer formation on larger, more relevant scales (Figure 6.5A).

More convenient access to the 3-bromopyrrole scaffold was provided by TIPS-Py.<sup>20-22</sup> Treatment of **17** with NBS, at low temperature (-78 °C), afforded **18** in good yield (70%), on multigram scales (>20 g). Further treatment of **18** with *n*BuLi at -78 °C, followed by addition of N-fluorobenzenesulfonimide gave fluorinated intermediate **19** in 50% yield on multigram scales. This transformation is very clean, as only two species, **17** and **19**, were detected in the crude reaction mixture. Similar results obtained with this reagent previously have attributed this limitation of yield to inherent side reactions of the fluorinating reagent. The obtained products proved to

difficult to separate, though cautious fractional distillation was somewhat successful (Figure 6.5B). With **19** in hand, two different routes to **1** were attempted, varying the order of nitro and ester introduction.

Nitration of **19** with  $\text{Cu(II)NO}_3$  gave **20** in modest yields, with good regioselectivity. The major by-product resulted from competing nitro-dehalogenation. It should be noted that 3-fluoro-4-nitropyrrole derivative **20** was stable over a span of weeks and did not require special handling conditions. Alternative nitration conditions, employing nitronium salts, were also examined; however, the observed regioselectivities were lower than for the method above and by-products resulting from desilylation were formed in significant quantities. The crude mixtures were purified by column chromatography, though 1-H derivatives like **21** were remarkably unstable, polymerizing upon standing or during chromatography (Figure 6.5C). Similar behavior was noted when **20** was intentionally desilylated with TBAF. In contrast, treatment of **19** with TBAF, followed by N-alkylation under phase transfer conditions gave **22**, albeit in low yield, after column chromatography. Trichloroacetylation of **22** gave a mixture of isomers, along with an assortment of by-products that did not contain fluorine. Successive column chromatography resulted in prohibitively low recoveries (Figure 6.5D).

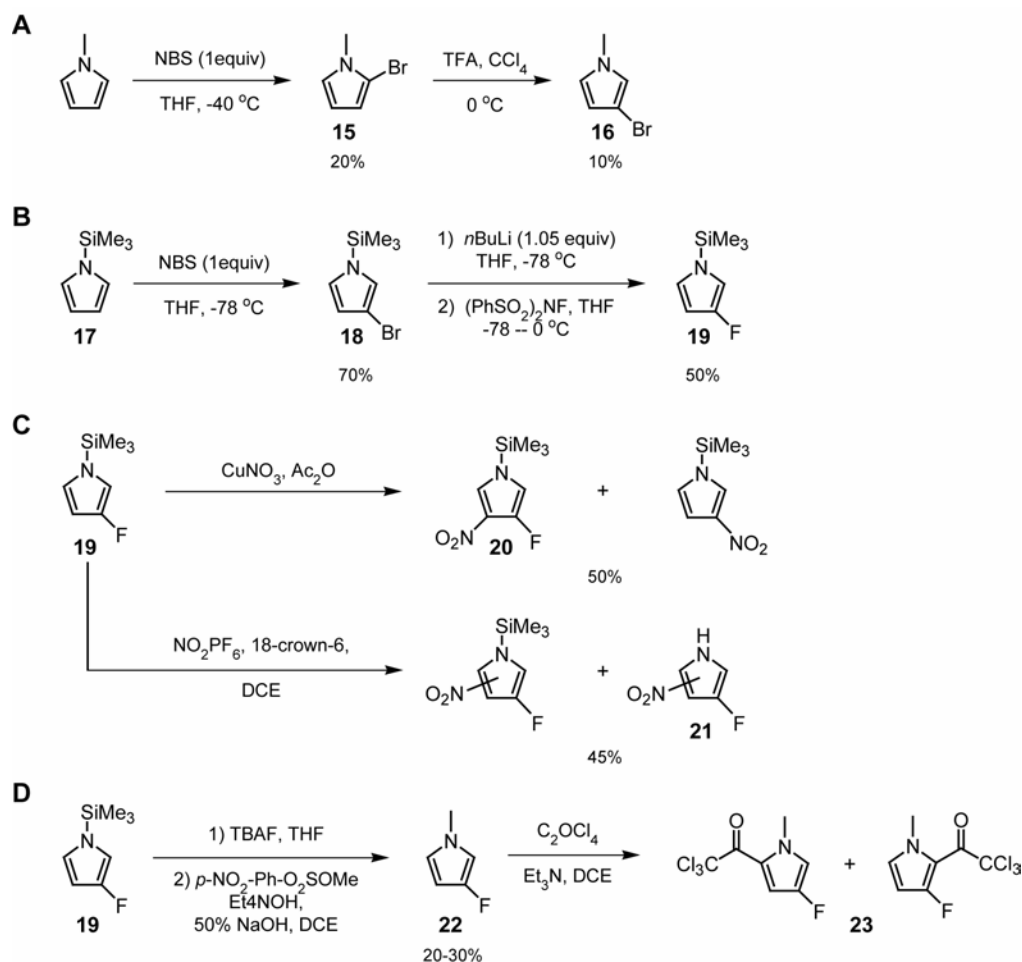


**Figure 6.5** Synthetic schemes to fluoropyrrole using electrophilic methods of aromatic fluorination. **(A)** Synthesis of 3-bromo-N-methylpyrrole from N-methylpyrrole starting material. **(B)** 3-Fluorination of TIPS-Py. **(C)** Examined synthetic routes to 3-fluoro-4-nitro-N-(TIPS)pyrrole. **(D)** Synthetic scheme installing the 2-ester moiety after the fluorine substituent.

Still other routes to Fp can be imagined, particular using a cyclization-based strategy to assemble ethyl 3-fluoro-N-methylpyrrole-2-carboxylate, **4**. This method would still require several steps to obtain intermediate **4** which must then be selectively nitrated at the  $\beta$ -position of a 1,2,3-trisubstituted pyrrole nucleus. This type of selectivity is simply not available, and separation of difficult mixtures of regioisomers, combined with low yields of desired product, make most any route to **1** a challenge. Xenon difluoride has been used to fluorinate polyamides directly,

however, 5-fluorination seems to be favored relative to 3-fluorination and verifying the regiochemistry of such a reaction would be incredibly inefficient. Given the vast array of chemical moieties that can be used as shape selective recognition elements and the suitability of other heterocycles as scaffolds for DNA recognition, the synthetic effort demanded by Fp seems to outweigh its potential benefits. Molecular modeling as well as the observed DNA-binding energetics of 3-fluorothiophene-2-carboxamide, described in Chapter 5A, support this notion.

### **Novel *Internal Residues from N-terminal Leads***

Before the nature of thiophene recognition in terminal pairings was contemplated, the thermodynamic data described in Chapter 5A encouraged the development of internal residues based upon N-terminal 3-methoxy- (Mt) and 3-chorothiophene-2-carboxamides (Ct). Internal derivatives were designed with the assumption that the sulfur atom was oriented toward the minor groove floor (Figure 6.6A). These residues proved difficult to prepare and were incorporated into solid phase techniques as dimers with Im (Figure 6.6B), due to the unreactive nature of their amino group (R. M. Doss, P. B. Dervan; unpublished results). Similar behavior has been noted in the preparation of 3-methylthiophene (Tn) monomers.<sup>11</sup>

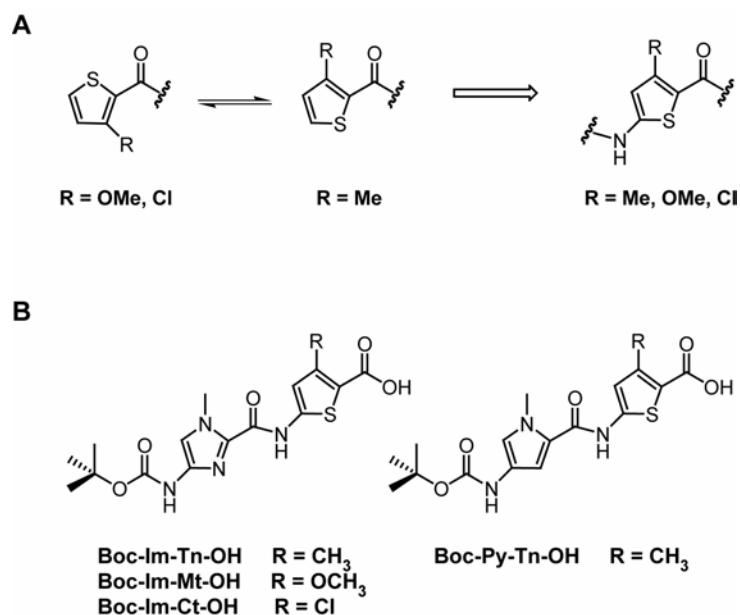


**Figure 6.6** Design of novel *internal* thiophene residues based upon leads from *N-terminal* studies. **(A)** Design rationale for internal thiophene residues. **(B)** Novel internal residues incorporated in solid phase polyamide synthesis as dimers.

Internal Mt and Ct residues did not exhibit the DNA recognition profiles expected based upon N-terminal results, while 3-methylthiophene residues behaved nearly identically in terminal and internal contexts (Table 6.1). A direct comparison of 3-substituent effects on DNA recognition by thiophene scaffolds in both *terminal* and *internal* pairings emphasizes the influence of context on specificity. One explanation for the context dependence evident above, involving rotation of terminal rings to alleviate repulsive intramolecular contacts, was discussed in Chapter 5A. A more detailed investigation of this hypothesis, using 2D-NMR, is underway in collaboration with the Wemmer group (University of California, Berkeley). The contrasting behavior of internal Mt and Ct residues does offer indirect support for the rotational hypothesis since the “sulfur down” conformation is enforced by internal

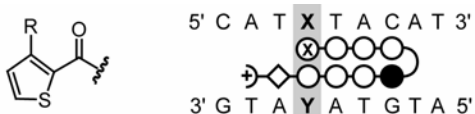


**Table 6.1A Observed  $K_a$  ( $M^{-1}$ ) for N-terminal 3-substituted-thiophene residues.<sup>a, b</sup>**

R	T • A	A • T	G • C	C • G
CH <sub>3</sub>	$2.3 \times 10^9 M^{-1}$	$1.4 \times 10^9 M^{-1}$	$\leq 10^7 M^{-1}$	$\leq 10^7 M^{-1}$
OCH <sub>3</sub>	$2.0 \times 10^9 M^{-1}$	$3.2 \times 10^8 M^{-1}$	$\leq 10^7 M^{-1}$	$\leq 10^7 M^{-1}$
Cl	$1.3 \times 10^{10} M^{-1}$	$3.9 \times 10^9 M^{-1}$	$3.1 \times 10^8 M^{-1}$	$2.1 \times 10^8 M^{-1}$

a) Values reported are the mean values from two DNase I footprinting titration experiments. b) Assays were performed at 22 °C in a buffer of 10 mM Tris.HCl, 10 mM KCl, 10 mM MgCl<sub>2</sub>, and 5 mM CaCl<sub>2</sub> at pH 7.0.



**Table 6.1B Observed  $K_a$  ( $M^{-1}$ ) for internal 3-substituted-thiophene residues.<sup>a, b</sup>**

R	T • A	A • T	G • C	C • G
CH <sub>3</sub>	$2.7 \times 10^9 M^{-1}$	$8.0 \times 10^8 M^{-1}$	$\leq 10^6 M^{-1}$	$\leq 10^6 M^{-1}$
OCH <sub>3</sub>	$9.0 \times 10^7 M^{-1}$	$9.5 \times 10^7 M^{-1}$	$\leq 10^6 M^{-1}$	$\leq 10^6 M^{-1}$
Cl	$2.1 \times 10^8 M^{-1}$	$8.1 \times 10^7 M^{-1}$	$\leq 10^6 M^{-1}$	$\leq 10^6 M^{-1}$

a) Values reported are the mean values from two DNase I footprinting titration experiments. b) Assays were performed at 22 °C in a buffer of 10 mM Tris.HCl, 10 mM KCl, 10 mM MgCl<sub>2</sub>, and 5 mM CaCl<sub>2</sub> at pH 7.0.

pairings. This places the 3-substituents proximal to the walls of the minor groove, lined by the phosphate backbone. Methyl substituents of Im, Py, and Tn residues are all tolerated; however, the greater steric demands of the chloro and methoxy groups may create unfavorable contacts with the minor groove walls or with substituents present on opposing aromatic residues (Figure 6.7).

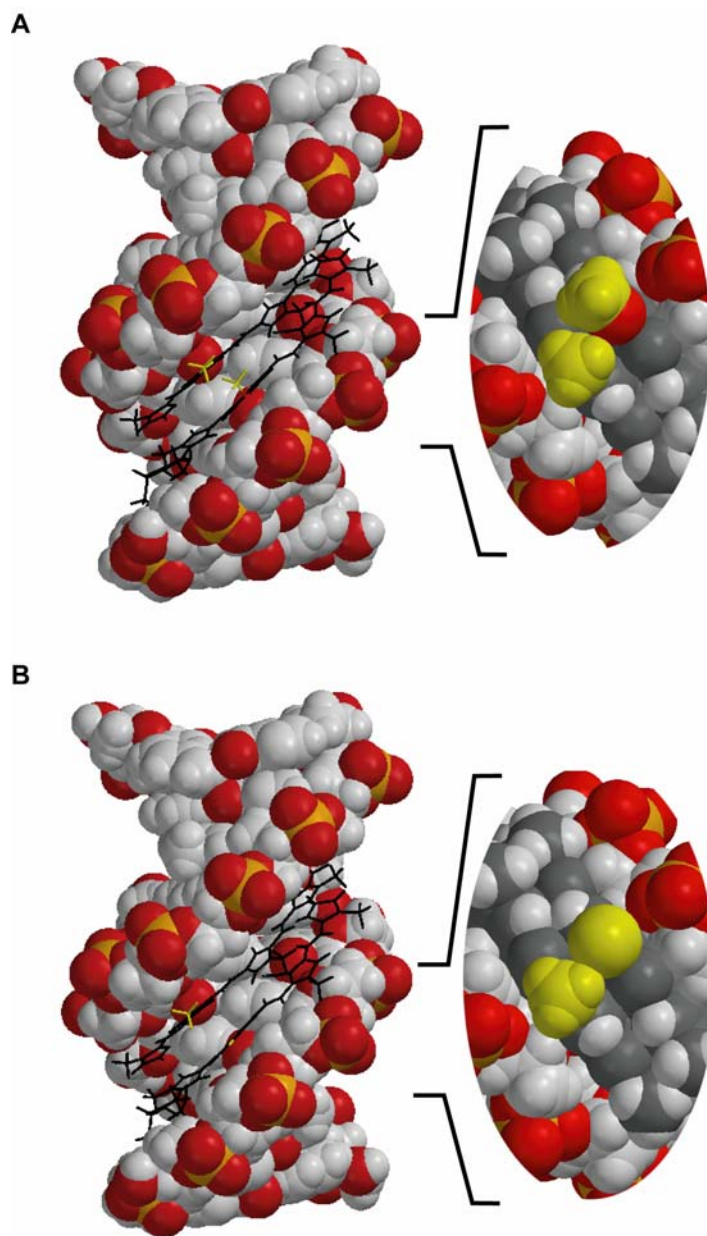
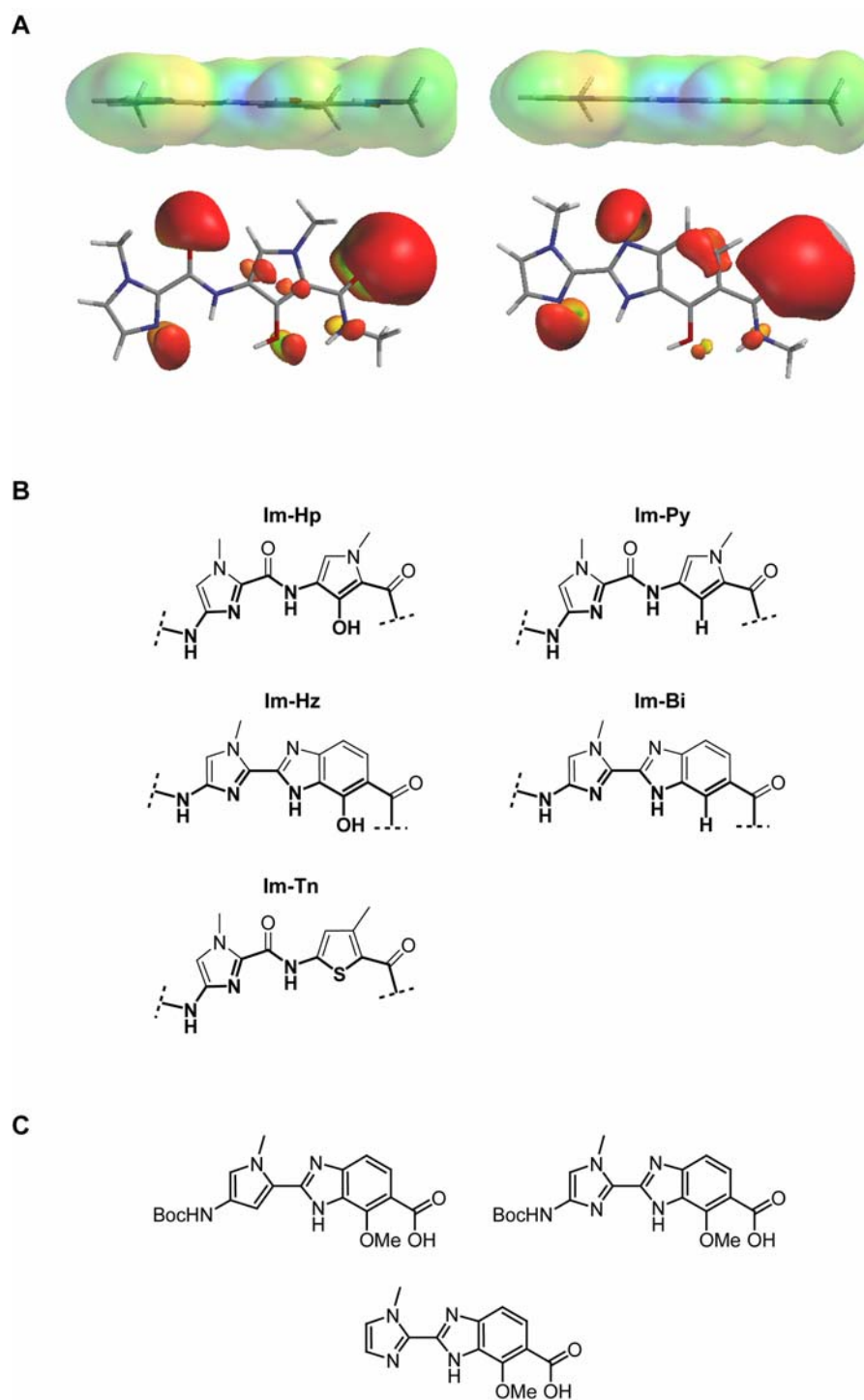


**Figure 6.7** Molecular rendering of unfavorable backbone interactions that could occur between internal 3-chloro- and 3-methoxy-thiophene residues when bound in the minor groove of DNA. **(A)** 3-methoxythiophene residue. **(B)** 3-chlorothiophene residue.

## Lead Candidates for Hp Replacement

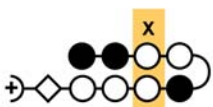
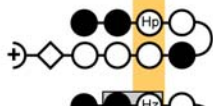
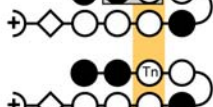
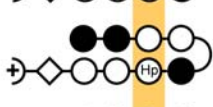
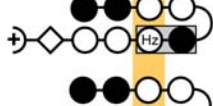
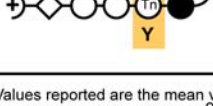
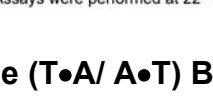
The most successful thymine-specific residues thus far developed as alternatives to internal Hp residues are 3-methylthiophene (Tn), discussed above, and hydroxybenzimidazole (Hz). The bicyclic architecture of Hz preserves the molecular shape and hydrogen bonding capacity of the minor groove-directed edge of the polyamide (Figure 6.8A). The direct linkage of the next residue to the benzimidazole ring also imposes constraints on the flexibility of the polyamide backbone while removing the 2-carboxamide oxygen. Despite the apparent differences in thymine-specific residues, the molecular surfaces they present to the minor groove are closely related (Figure 6.8B). The synthesis of Hz-containing polyamides, as dimers with Im or Py (Figure 6.8C), has been described previously and the DNA-binding properties of the thymine-selective rings above has been determined previously in the context of a single internal pairing (Table 6.2).<sup>14,15</sup>





**Figure 6.8** Benzimidazole scaffolds as internal Hp replacements. **(A)** Molecular models of Im-Py (*left*) and Im-Hz (*right*) dimers generated with Spartan. Electron densities are plotted over minimized equilibrium geometries. **(B)** Chemical structures of thymine-specific (*left*) ring systems attached to N-terminal Im and degenerate ring systems (*right*) attached to N-terminal Im. Bold edges represent the surface presented by the polyamide toward the minor groove floor. **(C)** Dimers used to incorporate novel benzimidazole residues into polyamides.

Table 6.2 Observed association constants ( $M^{-1}$ ) for Hp-, Tn-, and Hz-containing hairpin polyamides.<sup>a, b</sup>

Polyamide	T • A	A • T	G • C	C • G
	$4.7 (0.4) \times 10^9 M^{-1}$	$3.1 (0.7) \times 10^9 M^{-1}$	$2.2 (0.6) \times 10^8 M^{-1}$	$2.5 (0.9) \times 10^8 M^{-1}$
	$1.6 (0.3) \times 10^9 M^{-1}$	$8.1 (1.9) \times 10^7 M^{-1}$	$5.5 (1.5) \times 10^7 M^{-1}$	$7.9 (2.1) \times 10^7 M^{-1}$
	$5.5 (0.2) \times 10^9 M^{-1}$	$5.7 (0.4) \times 10^8 M^{-1}$	$\leq 1.0 \times 10^7 M^{-1}$	$\leq 1.0 \times 10^7 M^{-1}$
	$2.7 (0.2) \times 10^9 M^{-1}$	$8.0 (0.4) \times 10^8 M^{-1}$	$\leq 1.0 \times 10^6 M^{-1}$	$\leq 1.0 \times 10^6 M^{-1}$
	$9.8 (0.9) \times 10^7 M^{-1}$	$1.1 (0.2) \times 10^9 M^{-1}$	$2.5 (0.3) \times 10^7 M^{-1}$	$3.3 (1.0) \times 10^7 M^{-1}$
	$3.2 (0.6) \times 10^8 M^{-1}$	$1.4 (0.3) \times 10^9 M^{-1}$	$\leq 1.0 \times 10^7 M^{-1}$	$\leq 1.0 \times 10^7 M^{-1}$
	$5.4 (0.6) \times 10^9 M^{-1}$	$9.0 (0.5) \times 10^8 M^{-1}$	$\leq 1.0 \times 10^6 M^{-1}$	$\leq 1.0 \times 10^6 M^{-1}$

a) Values reported are the mean values from at least three DNase I footprinting titration experiments, with the standard deviation given in parentheses.  
 b) Assays were performed at 22 °C in a buffer of 10 mM Tris.HCl, 10 mM KCl, 10 mM MgCl<sub>2</sub>, and 5 mM CaCl<sub>2</sub> at pH 7.0.

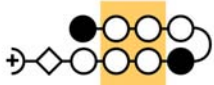
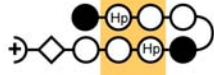
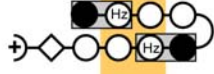
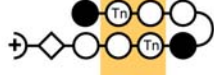



### Multiple (T•A/ A•T) Base Pair Recognition by Hairpin Polyamides

Thymine-specific internal residues complete the modular code for minor groove recognition, dramatically expanding the utility of polyamides in genomic settings. The DNA-recognition properties of Tn and Hz, paired opposite Py, as well as their chemical stabilities, offer substantial advantages relative to Hp. A full measure of the potential of these new residues; however, requires that their efficacy in targeting multiple (T•A/ A•T) base pairs, in the context of single binding site, be determined. Thus far, pairings of Im with Py are the standard for comparison in this context.

Hairpin polyamides containing adjacent pairings of Tn or Hz with Py were screened for binding to containing TA, AA, and AT core sequences. This data, as

well as the corresponding results for Hp-containing polyamides is summarized in Table 6.3. It should be noted that neither Tn or Hz can be used to target the central AA site. The Tn-Tn dimer required for synthesis of such a polyamide has proved synthetically intractable in our hands and Hz is inherently unsuited to targeting adjacent thymine bases.

**Table 6.3 Observed association constants ( $M^{-1}$ ) for multiple Hp-, Tn-, and Hz-containing hairpin polyamides.<sup>a, b</sup>**

Polyamide	5'-aGTACT-3'	5'-aGAACt-3'	5'-aGATCt-3'
	$3.5 (0.7) \times 10^{10} M^{-1}$	$4.7 (0.7) \times 10^9 M^{-1}$	$7.4 (1.5) \times 10^8 M^{-1}$
	$7.0 (1.8) \times 10^8 M^{-1}$	$\leq 1.0 \times 10^7 M^{-1}$	$\leq 1.0 \times 10^7 M^{-1}$
	$4.6 (0.8) \times 10^8 M^{-1}$	$3.2 (0.4) \times 10^7 M^{-1}$	$1.7 (0.5) \times 10^7 M^{-1}$
	$1.0 (0.5) \times 10^8 M^{-1}$	$1.0 (0.3) \times 10^8 M^{-1}$	$1.0 (0.4) \times 10^8 M^{-1}$
	$1.0 (0.2) \times 10^8 M^{-1}$	$2.6 (0.6) \times 10^7 M^{-1}$	$3.3 (0.7) \times 10^7 M^{-1}$
	$4.5 (0.7) \times 10^8 M^{-1}$	$3.3 (0.7) \times 10^8 M^{-1}$	$4.4 (0.9) \times 10^8 M^{-1}$
	$3.3 (0.9) \times 10^8 M^{-1}$	$4.7 (0.6) \times 10^8 M^{-1}$	$4.5 (0.7) \times 10^8 M^{-1}$

a) Values reported are the mean values from at least three DNase I footprinting titration experiments, with the standard deviation given in parentheses.  
 b) Assays were performed at 22 °C in a buffer of 10 mM Tris.HCl, 10 mM KCl, 10 mM MgCl<sub>2</sub>, and 5 mM CaCl<sub>2</sub> at pH 7.0.

The results in Table 6.3 illustrate the potential advantages and disadvantages inherent to the strategies used in novel internal residue development. While individual Tn/Py pairings offer modest selectivity for T•A with high affinity, multiple pairings within a given polyamide lead to loss of specificity and coating, at higher concentrations. The shape selective mode of Tn recognition may cause distortions in the double helix and combinations of this effect in the multiple context might be

responsible for widening of the minor groove such that intimate physical contacts are lost, leading to loss of specificity. The properties of Hz, relative to Py, are encouraging. Specificity multiple of Hz/Py pairings is at least comparable to Hp/Py, if not slightly lower, but affinities are consistently higher, suggesting that Hz might serve as useful replacement for Hp in biological applications.

**References**

- 1) Dervan, P. B. *Bioorg. Med. Chem.* **2001**, *9*, 2215.
- 2) Mrksich, M.; Wade, W. S.; Dwyer, T. J.; Geierstanger, B. H.; Wemmer, D. E.; Dervan, P. B. *Proc. Natl. Acad. Sci. USA* **1992**, *89*, 7586.
- 3) Kielkopf, C. L.; Baird, E. E.; Dervan, P. B.; Rees, D. C. *Nat. Struct. Biol.* **1998**, *5*, 104.
- 4) White, S.; Szewczyk, J. W.; Turner, J. M.; Baird, E. E.; Dervan, P. B. *Nature* **1998**, *391*, 468.
- 5) Wade, W. S.; Mrksich, M.; Dervan, P. B. *J. Am. Chem. Soc.* **1992**, *114*, 8783.
- 6) Kielkopf, C. L.; White, S.; Szewczyk, J. W.; Turner, J. M.; Baird, E. E.; Dervan, P. B.; Rees, D. C. *Science* **1998**, *282*, 111.
- 7) Kielkopf, C. L.; Bremer, R. E.; White, S.; Szewczyk, J. W.; Turner, J. M.; Baird, E. E.; Dervan, P. B.; Rees, D. C. *J. Mol. Biol.* **2000**, *295*, 557.
- 8) Wellenzohn, B.; Loferer, M. J.; Trieb, M.; Rauch, C.; Winger, R. H.; Mayer, E.; Liedl, K. R. *J. Am. Chem. Soc.* **2003**, *125*, 1088.
- 9) White, S.; Turner, J. M.; Szewczyk, J. W.; Baird, E. E.; Dervan, P. B. *J. Am. Chem. Soc.* **1999**, *121*, 260.
- 10) Melander, C.; Herman, D. M.; Dervan, P. B. *Chem. Eur. J.* **2000**, *24*, 4487.
- 11) Marques, M. A.; Doss, R. M.; Urbach, A. R.; Dervan, P. B. *Helv. Chim. Acta.* **2002**, *85*, 4485.
- 12) Foister, S.; Marques, M. A.; Doss, R. M.; Dervan, P. B. *Bioorg. Med. Chem.*  
**In press.**
- 13) Minehan, T. G.; Gottwald, K.; Dervan, P. B. *Helv. Chim. Acta.* **2000**, *83*, 2197.

- 14) Briehn, C. A.; Weyermann, P.; Dervan, P. B. *Chem. Eur. J.* **2003**, *9*, 2110.
- 15) Renneberg, D.; Dervan, P. B. *J. Am. Chem. Soc.* **2003**, *125*, 5707.
- 16) Clark, J. H.; Wails, D.; Bastock, T. W. *Aromatic Fluorination*; CRC Press: New York, 1996.
- 17) Gilow, H.M.; Burton, D. E. *J. Org. Chem.* **1981**, *46*, 2221.
- 18) Carmona, O.; Greenhouse, R.; Landeros, R.; Muchowski, J.M. *J. Org. Chem.* **1980**, *45*, 5336.
- 19) Carson, J. R.; Davis, N. M. *J. Org. Chem.*, **1981**, *46*, 839.
- 20) Bray, B. L.; Mathies, P. H.; Naef, R.; Solas, D. R.; Tidwell, T. T.; Artis, D. R.; Muchowski, J. M. *J. Org. Chem.* **1990**, *55*, 6317.
- 21) Lal, G. S.; Pez, G. P.; Syvret, R. G. *Chem. Rev.* **1996**, *96*, 1737.
- 22) Guk, Y. V.; Ilyushin, M. A.; Golod, E. L.; Gidaspov, B. V. *Russ. Chem. Rev.* **1983**, *52*, 284.